CBPF-NF-015/00

Focusing Vacuum Fluctuations

L.H. Ford[1]

Institute of Cosmology, Department of Physics and Astronomy
Tufts University
Medford, Massachusetts 02155

N.F. Svaiter[2]

Centro Brasileiro de Pesquisas Fisicas-CBPF
Rua Dr. Xavier Sigaud 150
Rio de Janeiro, RJ 22290-180, Brazil

Abstract

The focusing of the vacuum modes of a quantized field by a parabolic mirror is investigated. We use a geometric optics approximation to calculate the energy density and mean squared field averages for scalar and electromagnetic fields near the focus. We find that these quantities grow as an inverse power of the distance to the focus. There is an attractive Casimir-Polder force on an atom which will draw it into the focus. Some estimates of the magnitude of the effects of this focusing indicate that it may be observable.

PACS categories: 03.70.+k, 34.20.Cf, 12.20.Ds, 04.62.+v.

[1]email: ford@cosmos2.phy.tufts.edu
[2]email:nfuxsvai@lafex.cbpf.br

1 Introduction

The Casimir effect can be viewed as the reflection of vacuum fluctuations by mirrors. The presence of a reflecting boundary alters the modes of a quantized field, and results in shifts in the vacuum expectation values of quantities quadratic in the field, such as the energy density. Typically, Casimir effects for massless fields may be estimated by dimensional analysis. If r is the distance to the nearest boundary, then the Casimir energy density is typically of order r^{-4} times a dimensionless constant. This constant is usually of order 10^{-3} in four-dimensional spacetime. It is of course possible to find a much smaller result due to special cancellations. For example, the Casimir energy density for a single, perfectly conducting plate is zero, even though the mean squared electric and mean squared magnetic fields are separately nonzero.

However, these typical results arise from calculations of specific geometries, not from any general theorem. This leaves the possibility of exceptions, where the energy density is much larger than would be expected on dimensional grounds. Indeed, one possible mechanism for amplification of vacuum fluctuations has already been proposed [1, 2]. This mechanism is based on the fact that the contribution of various parts of the frequency spectrum to the Casimir effect is a highly oscillatory function [3, 4]. The contributions of different ranges of frequency almost, but not quite, completely cancel one another. This opens the possibility that one can inhance the magnitude of the effect by altering the reflectivity of the boundary in selected frequency ranges.

In this paper, we wish to propose a different mechanism for amplification of vacuum fluctuations. This is the use of parabolic mirrors to create anomalously large effects near the mirror's focus. It is well known in classical physics that a parabolic mirror can focus incident rays which are parallel to the mirror's axis. This means that a particular plane wave mode becomes singular at the focus. One might wonder if this classical effect on modes produces large vacuum fluctuations near the focus. We will argue that the answer to this question is yes.

The outline of this paper is as follows: In Sect. 2, the essential formalism needed to compute mean squared field averages in the geometric optics approximation will be developed. It will be argued that the dominant contributions will come from interference terms between different reflected rays. In particular, expressions will be given for the case of two reflected rays from a single incident ray in terms of the path length difference of the two reflected rays. In Sect. 3 the specific case of parabolic mirrors will be studied, and the condition for the existence of multiply reflected rays given. It will be shown here that there is a minimum size required for a parabolic mirror to produce large vacuum fluctuation focusing. Section 4 deals with a couple of technical issues, including the treatment of the apparently singular integrals which arise. In Sect. 5, we give explicit results in an approximation in which the mirror is only slightly larger than the minimum size needed to focus vacuum fluctuations. The possible experimental tests of these results are discussed in Sect. 6, and conclusions are given in Sect. 7.

Units in which $\hbar = c = 1$ will be used throughout this paper. Electromagnetic quantites will be in Lorentz-Heaviside units.

2 Basic Formalism

The approach which will be adopted in this paper is a geometric optics approximation. This approximation assumes that the dominant contribution to the quantities which we calculate comes from modes whose wavelengths are short compared to the goemetric length scales of the system. The justification of the approximation will lie in a self-consistent calculation leading to large contributions from short wavelength modes. At first sight, it might seem that this approximation would always fail, and that only modes whose wavelengths are of the order of the goemetric length scales will contribute significantly to quantities such Casimir energy densities. However, there is a circumstance in which this intuition can fail. This is when there are two or more reflected rays produced by the same incident beam. It then becomes possible to have an anomalously large interference term between these rays, as will be illustrated below.

Let us first consider the case of a massless scalar field, φ. Let the field operator be expanded in term of normal modes as

$$\varphi = \sum_{\mathbf{k}} (a_{\mathbf{k}}\, F_{\mathbf{k}} + a^{\dagger}_{\mathbf{k}}\, F^{*}_{\mathbf{k}})\,, \tag{1}$$

where $a^{\dagger}_{\mathbf{k}}$ and $a_{\mathbf{k}}$ are creation and annihilation operators, and $F_{\mathbf{k}}$ are the mode functions. The formal vacuum expectation value of φ^2 becomes

$$\langle \varphi^2 \rangle_f = \sum_{\mathbf{k}}\, |F_{\mathbf{k}}|^2\,. \tag{2}$$

In the absence of a boundary, the modes $F_{\mathbf{k}}$ are simply plane waves. In the presence of the boundary, there are both incident and possibly one or more reflected waves for each wave vector $\mathbf{k}$. Write the mode function as

$$F_{\mathbf{k}} = f_{\mathbf{k}} + \sum_i f^{(i)}_{\mathbf{k}}\,, \tag{3}$$

where $f_{\mathbf{k}}$ is the incident wave and the $f^{(i)}_{\mathbf{k}}$ are the reflected waves. (Note that here $\mathbf{k}$ denotes the incident wavevector.) We may take all of these waves to be plane waves with box normalization in a volume V, in which case

$$f_{\mathbf{k}} = \frac{1}{\sqrt{2\omega V}}\, \mathrm{e}^{i(\mathbf{k}\cdot\mathbf{x}-\omega t)}\,. \tag{4}$$

The $f^{(i)}_{\mathbf{k}}$ take the same form, but with $\mathbf{k}$ replaced by the appropriate wavevector for the reflected wave.

If we now insert Eq. (3) into Eq. (2), we obtain a sum involving both the absolute squares of the incident and the reflected waves, and the various possible cross terms between the different waves:

$$\langle \varphi^2 \rangle_f = \sum_{\mathbf{k}} \left[|f_{\mathbf{k}}|^2 + \sum_i |f^{(i)}_{\mathbf{k}}|^2 + \sum_i (f^{*}_{\mathbf{k}} f^{(i)}_{\mathbf{k}} + f_{\mathbf{k}} {f^{(i)}}^{*}_{\mathbf{k}}) + \sum_{i\neq j} f^{(i)}_{\mathbf{k}} {f^{(j)}}^{*}_{\mathbf{k}} \right]\,. \tag{5}$$

This quantity is divergent and needs to be renormalized by subtraction of the corresponding quantity in the absence of boundaries. We will argue in Sect. 4.1 that this is given by the above sum without the cross terms:

$$\langle\varphi^2\rangle_0 = \sum_{\mathbf{k}} (|f_{\mathbf{k}}|^2 + \sum_i |f^{(i)}_{\mathbf{k}}|^2) \,. \tag{6}$$

The renormalized expectation value is then given by the sum of cross terms

$$\langle\varphi^2\rangle = \langle\varphi^2\rangle_f - \langle\varphi^2\rangle_0 = \sum_{\mathbf{k}} \left[\sum_i (f^*_{\mathbf{k}} f^{(i)}_{\mathbf{k}} + f_{\mathbf{k}} {f^{(i)}}^*_{\mathbf{k}}) + \sum_{i\neq j} f^{(i)}_{\mathbf{k}} {f^{(j)}}^*_{\mathbf{k}} \right] \,. \tag{7}$$

Let us examine a particular cross term:

$$T_{12} = \sum_{\mathbf{k}} (f^{(1)}_{\mathbf{k}} {f^{(2)}}^*_{\mathbf{k}} + f^{(2)}_{\mathbf{k}} {f^{(1)}}^*_{\mathbf{k}}) \,. \tag{8}$$

Here $f^{(1)}_{\mathbf{k}}$ and $f^{(2)}_{\mathbf{k}}$ are both of the form of Eq. (4), except with $\mathbf{k}$ replaced by $\mathbf{k}_1$ and $\mathbf{k}_2$, respectively. These might be two reflected waves, both corresponding to the same incident wavevector $\mathbf{k}$, but different reflected wavevectors, $\mathbf{k}_1$ and $\mathbf{k}_2$. Only the direction, not the frequency changes upon reflection, so

$$|\mathbf{k}_1| = |\mathbf{k}_2| = |\mathbf{k}| = \omega \,. \tag{9}$$

We can now write

$$T_{12} = 2\,\mathrm{Re} \sum_{\mathbf{k}} \frac{1}{2\omega V}\, \mathrm{e}^{i[\mathbf{k}_1 - \mathbf{k}_2)\cdot\mathbf{x}} \to \frac{1}{8\pi^2} \int d^3k \frac{\cos[(\mathbf{k}_1 - \mathbf{k}_2)\cdot\mathbf{x}]}{\omega} \,, \tag{10}$$

where the infinite volume limit has been taken. The argument of the cosine function is proportional to the difference in optical path lengths of the two rays, $\Delta\ell$, so that

$$(\mathbf{k}_1 - \mathbf{k}_2)\cdot\mathbf{x} = \omega\,\Delta\ell \,, \tag{11}$$

and hence

$$T_{12} = \frac{1}{8\pi^2} \int d^3k \, \frac{\cos\omega\,\Delta\ell}{\omega} \,. \tag{12}$$

Note that the integral in the above expression will diverge as $(\Delta\ell)^{-2}$ in the limit that $\Delta\ell \to 0$. Thus within the geometric optics approximation, we can obtain an anomalously large contribution if there are two distinct reflected rays with nearly the same optical path length. If this is the case, it provides the self-consistent justification of the approximation. The dominant contribution to the integral will come from modes with wavelength of the order of $\Delta\ell$; if this is small compared to all other length scales in the problem, then the use of geometric optics should be a good approximation.

In this paper, we will examine the case of parabolic mirrors and show that for points near the focus, there can be two reflected rays with nearly the same path length. Their path lengths differ finitely from that of the incident ray. In this case, the dominant contribution to $\langle\varphi^2\rangle$ comes from a single term of the form of T_{12}, and we can write

$$\langle\varphi^2\rangle \approx \frac{1}{8\pi^2} \int d^3k \, \frac{\cos\omega\,\Delta\ell}{\omega} \,. \tag{13}$$

Note that the interference terms between the incident and the reflected rays give a much smaller contribution because the $\Delta\ell$ is much larger for these terms. We can also now write down expressions for several other quantities of interest. These include $\langle\dot{\varphi}^2\rangle$, where the dot denotes a time derivative, as well as the scalar field energy density

$$\rho_{scalar} = \frac{1}{2}\langle\dot{\varphi}^2 + |\nabla\varphi|^2\rangle \approx \langle\dot{\varphi}^2\rangle \,. \tag{14}$$

In the last step we used the fact that

$$|\dot{f}^{(i)}_{\mathbf{k}}| = |\nabla f^{(i)}_{\mathbf{k}}| \tag{15}$$

for plane wave modes. We can also obtain renormalized expectation values for electromagnetic field quantities, such as $\langle\mathbf{E}^2\rangle$ and $\langle\mathbf{B}^2\rangle$, or the electromagnetic energy density $\rho_{EM} = \frac{1}{2}(\langle\mathbf{E}^2\rangle + \langle\mathbf{B}^2\rangle)$. Here $\mathbf{E}$ and $\mathbf{B}$ are the quantized electric and magnetic field operators, respectively. The mode functions for these fields are of the form of the right-hand-side of Eq. (4), except with an extra factor of ω and a unit polarization vector. Thus, when we account for the two polarizations of the electromagnetic field, we have

$$\langle\mathbf{E}^2\rangle = \langle\mathbf{B}^2\rangle = \rho_{EM} = 2\langle\dot{\varphi}^2\rangle = 2\rho_{scalar} = \frac{1}{4\pi^2}\int d^3k\,\omega\,\cos\omega\,\Delta\ell\,. \tag{16}$$

3 Optics of Parabolic Mirrors

3.1 Conditions for Multiply Reflected Rays

A parabolic mirror is illustrated in Fig. 1. The parabola described by

$$x = \frac{b^2 - y^2}{2b} \tag{17}$$

has its focus at the origin, $x = y = 0$. Consider a ray incident at angle θ and reflected at angle θ' relative to the x-axis. Further suppose that this ray reaches the x-axis at $x = a$, where $a \ll b$. We wish to find the relationship between the angles θ and θ'. First note that

$$\theta = \theta' - \pi + 2\alpha\,, \tag{18}$$

where α is the angle of the tangent to the parabola at the point of intersection. If we differentiate Eq. (17), we find

$$\frac{dy}{dx} = -\frac{b}{y_i} = -\tan\alpha\,, \tag{19}$$

where here y_i is the y-coordinate of the point of reflection. Note that the reflected ray is described by

$$y = \tan\theta'\,(x - a)\,. \tag{20}$$

Combine this relation with Eq. (17) to find

$$y_i = -\frac{b}{\tan\theta'}\left[1 \pm \sqrt{\sec^2\theta' - 2\left(\frac{a}{b}\right)\tan^2\theta'}\right]\,. \tag{21}$$

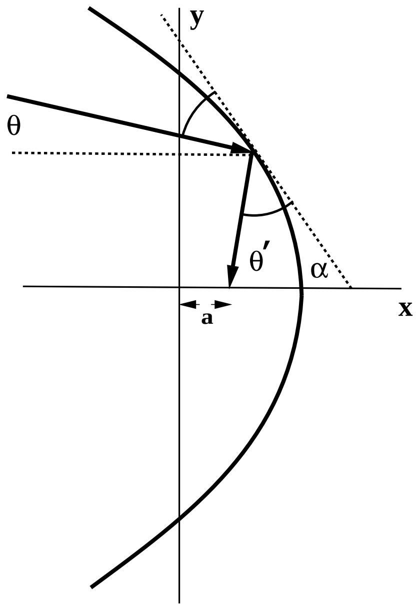

Figure 1: A parabolic mirror has its focus at the origin. A ray incident at an angle θ with respect to the x-axis reflects off the mirror and arrives at a point a distance a from the origin at an angle θ'. The line tangent to the point of reflection is at an angle α.

We expand this expression to first order in a/b and note that for $y_i > 0$, we need the minus sign before the square root. We then find

$$y_i \approx -\frac{b}{\tan\theta'}\left[1-\sec\theta' + \left(\frac{a}{b}\right)\sin^2\theta'\sec\theta'\right] . \tag{22}$$

Now combine this result with Eqs. (18) and (19) to find, to first order in a/b,

$$\theta = \frac{a\,\sin^3\theta'\,\sec\theta'}{b(\sec\theta'-1)} . \tag{23}$$

First, we note that $\theta \to 0$ as $a \to 0$ for fixed θ'. This is the expected result that all rays emanating from the focus are reflected into parallel rays. Equation (23) is plotted in Fig. 2. We see that for $a \neq 0$, there can be two reflected rays for a given incident ray. However, one of the reflected rays always corresponds to $\theta' > \pi/3$. Hence the mirror must subtend an angle greater than $\pi/3$ as measured from the x-axis for this to happen.

Our next task is to compute the difference in path lengths for these two reflected rays. Consider first the distance ℓ which a particular ray travels after it first crosses the line $x = a$. This distance can be broken into two segments s_1 and s_2, as illustrated in Fig. 3. If x_i is the x-coordinate of the reflection point, then

$$s_1 = \sqrt{(x_i - a)^2 + y_i^2} \tag{24}$$

and

$$s_2 = \frac{x_i - a}{\cos\theta} . \tag{25}$$

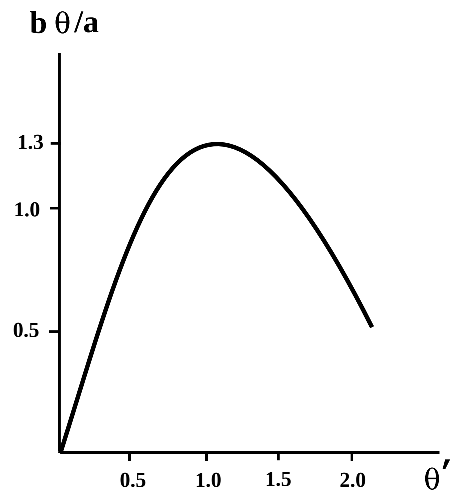

Figure 2: The incident angle θ as a function of the angle θ' of the reflected ray. Here it is assumed that the rays arrive near the focus ($a/b \ll 1$). For a single incident angle θ, there can be two reflection angles θ'. The maximum of this curve occurs at $\theta' = \pi/3$.

We may now use Eqs. (17) and (21) to write

$$s_1 \approx \frac{b}{\sin^2\theta'}\left[1 - \cos\theta' - \left(\frac{a}{b}\right)\sin^2\theta'\right]. \tag{26}$$

Similarly,

$$s_2 \approx x_i - a \approx \frac{b\,\cos\theta'}{\sin^2\theta'}\left[1 - \cos\theta' - \left(\frac{a}{b}\right)\sin^2\theta'\right]. \tag{27}$$

Thus,

$$\ell = s_1 + s_2 = b - a(1 + \cos\theta'). \tag{28}$$

If there are two distinct reflected rays with $\theta' = \theta'_1$ and $\theta' = \theta'_2$, respectively, then the path length difference is

$$\Delta\ell = a(\cos\theta'_1 - \cos\theta'_2). \tag{29}$$

3.2 Parabola of Revolution

In Section 3, we dealt with the rays reflected from a parabola in a plane. There are two ways to add on the third spatial dimension. One is to consider a parabolic cylinder and the other is to consider a parabola of revolution, the surface formed by rotating a parabola about its symmetry axis. In the latter case, one has an azimuthal angle $0 \leq \phi < 2\pi$. Thus Eq. (13) becomes

$$\langle\varphi^2\rangle_{pr} = \frac{1}{4\pi^2}\int d\theta' \int_0^\infty d\omega\,\omega\cos\omega\,\Delta\ell = -\frac{1}{4\pi^2 a^2}\int d\theta'\,\frac{1}{(\cos\theta'_1 - \cos\theta'_2)^2}. \tag{30}$$

Here we have evaluated

$$\int_0^\infty d\omega\,\omega\cos\omega\,\Delta\ell = \lim_{\alpha\to 0}\int_0^\infty d\omega\,\omega\cos\omega\Delta\ell\;\mathrm{e}^{-\alpha\omega} = -\frac{1}{\Delta\ell^2}, \tag{31}$$

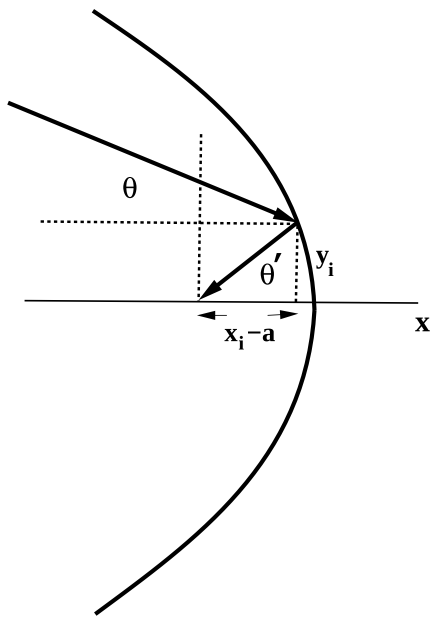

Figure 3: The ray reflects from a point on the mirror with coordinates (x_i, y_i) and then arrives at the point $(a, 0)$.

and then used Eq. (29).

We can do an analogous calculation for the various quantites given in Eq. (16) to find, for example,

$$\langle \mathbf{E}^2 \rangle_{pr} = \frac{3}{2\pi^2 a^4} \int d\theta' \, \frac{1}{(\cos\theta'_1 - \cos\theta'_2)^4} \,. \tag{32}$$

Here we have used

$$\int_0^\infty d\omega\, \omega^3 \cos\omega\, \Delta\ell = \lim_{\alpha \to 0} \int_0^\infty d\omega\, \omega^3 \cos\omega \Delta\ell \, \mathrm{e}^{-\alpha\omega} = \frac{6}{(\Delta\ell)^4} \,. \tag{33}$$

3.3 Parabolic Cylinder

Another possible geometry in three space dimensions is that of the parabolic cylinder. Let the cylinder be parallel to the z-direction. The wavevector $\mathbf{k}$ of the light rays now has a z-component, k_z, so that

$$\omega = \sqrt{\kappa^2 + k_z^2} \,, \tag{34}$$

where κ is the magnitude of the component of $\mathbf{k}$ in the xy plane (perpendicular to the z-direction). If s is a distance traveled in the xy plane, then the actual distance traveled is

$$\sigma = s \, \frac{\omega}{\kappa} \,. \tag{35}$$

Thus the difference in path lengths for a pair of reflected rays is $\omega\, \Delta\ell / \kappa$. We can modify Eq. (13) to give an expression for the mean value of φ^2 near the focus of a parabolic cylinder as

$$\langle\varphi^2\rangle_{pc} = \frac{1}{8\pi^3}\int d^3k\,\frac{\cos(\omega^2\,\Delta\ell/\kappa)}{\omega}\,. \tag{36}$$

Similarly, the mean squared electric field is given by the analog of Eq. (16):

$$\langle\mathbf{E}^2\rangle_{pc} = \frac{1}{4\pi^3}\int d^3k\,\omega\,\cos(\omega^2\,\Delta\ell/\kappa)\,. \tag{37}$$

The integrations in these two expressions are best done in cylindrical coordinates, where $d^3k = \kappa\,d\kappa\,d\theta'\,dk_z$. We can then write

$$\begin{aligned}\langle\varphi^2\rangle_{pc} &= \frac{1}{8\pi^3}\int d\theta'\int_0^\infty d\kappa\,\kappa\,\mathrm{Re}\left(\mathrm{e}^{i\kappa\Delta\ell}\int_{-\infty}^\infty \frac{dk_z}{\sqrt{\kappa^2+k_z^2}}\,\mathrm{e}^{i\Delta\ell\,k_z^2/\kappa}\right)\\ &= \frac{1}{8\pi^3}\int d\theta'\,\mathrm{Re}\int_0^\infty d\kappa\,\kappa\,\mathrm{e}^{\frac{1}{2}i\kappa\Delta\ell}\,K_0\left(-\frac{1}{2}i\kappa\Delta\ell\right)\,,\end{aligned} \tag{38}$$

where K_0 is a modified Bessel function, and in the last step we used Formula 3.364.3 in Ref. [5]. Next we use Formula 6.624.1 in the same reference to write

$$\begin{aligned}\lim_{\alpha\to\beta}\int_0^\infty dx\,x\,\mathrm{e}^{-\alpha x}K_0(\beta x) &= \lim_{\alpha\to\beta}\left(\frac{1}{\alpha^2-\beta^2}\left\{\frac{\alpha}{\sqrt{\alpha^2-\beta^2}}\ln\left[\frac{\alpha}{\beta}+\sqrt{\left(\frac{\alpha}{\beta}\right)^2-1}\right]-1\right\}\right)\\ &= \frac{1}{3\beta^2}\,.\end{aligned} \tag{39}$$

We can combine this last result with Eqs. (30) and (38) to write

$$\langle\varphi^2\rangle_{pc} = \frac{2}{3\pi}\,\langle\varphi^2\rangle_{pr}\,. \tag{40}$$

Similarly, we can write

$$\begin{aligned}\langle\mathbf{E}^2\rangle_{pc} &= \frac{1}{4\pi^3}\int d\theta'\int_0^\infty d\kappa\,\kappa^2\,\frac{d}{d\,\Delta\ell}\int_{-\infty}^\infty \frac{dk_z}{\sqrt{\kappa^2+k_z^2}}\sin\left(\frac{\kappa^2+k_z^2}{\kappa}\,\Delta\ell\right)\\ &= \frac{1}{4\pi^3}\int d\theta'\,\frac{d}{d\,\Delta\ell}\,\mathrm{Im}\int_0^\infty d\kappa\,\kappa^2\,\mathrm{e}^{\frac{1}{2}i\kappa\Delta\ell}\,K_0\left(-\frac{1}{2}i\kappa\Delta\ell\right)\,.\end{aligned} \tag{41}$$

If we differentiate Eq. (39) with respect to α before taking the limit, we may show that

$$\lim_{\alpha\to\beta}\int_0^\infty dx\,x^2\,\mathrm{e}^{-\alpha x}K_0(\beta x) = \frac{4}{15\beta^3}\,. \tag{42}$$

This last identity and Eq. (16) may be used to show that

$$\langle\mathbf{E}^2\rangle_{pc} = \frac{8}{15\pi}\,\langle\mathbf{E}^2\rangle_{pr}\,. \tag{43}$$

Thus the results for the parabolic cylinder are related to those for the parabola of revolution by a numerical factor somewhat less than unity.

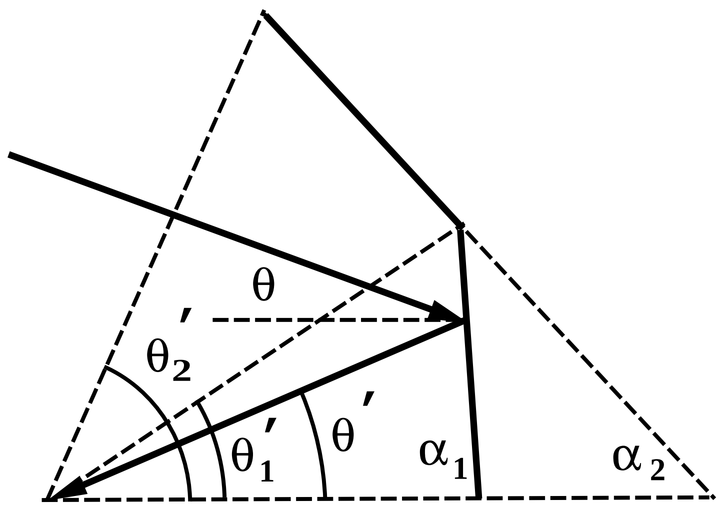

Figure 4: Two flat mirror segments are aligned at angles α_1 and α_2, respectively, and subtend angles θ'_1 and $\theta'_2 - \theta'_1$ from the point of interest. An incident ray has angle θ with respect to the x-axis, whereas the reflected ray has angle θ'.

4 Further Technical Issues

4.1 Reflected Rays from Line Segments

In this subsection, we examine the problem of the reflection of rays from a pair of attached line segments, as illustrated in Fig. 4. The purpose of this exercise is twofold: First, it will lead to the justification of the renormalization prescription used in writing down Eq. (6). Second, it will reveal that integrals such as those in Eqs. (7) and (16) should involve an integration over θ', the angle of the reflected wave, rather than θ, the angle of the incident wave.

First consider the case $0 < \theta' < \theta'_1$, so the ray reflects from the lower segment oriented at angle α_1 relative to the horizontal. Here $\theta = \theta' + 2\alpha_1 - \pi$ and hence

$$2\alpha_1 - \pi < \theta < \theta'_1 + 2\alpha_1 - \pi \,. \tag{44}$$

Now consider the case where the ray reflects from the upper segment, so $\theta'_1 < \theta' < \theta'_2$ and $\theta = \theta' + 2\alpha_2 - \pi$. Here

$$\theta'_1 + 2\alpha_2 - \pi < \theta < \theta'_2 + 2\alpha_2 - \pi \,. \tag{45}$$

Note that the range of θ' is $\Delta\theta' = \theta'_2$ whereas the range of θ is

$$\Delta\theta = \theta'_2 + 2(\alpha_2 - \alpha_1) < \theta'_2 \,. \tag{46}$$

However, for θ in the range $\theta'_1 + 2\alpha_2 - \pi < \theta < \theta'_1 + 2\alpha_1 - \pi$, there are two reflected rays for each incident ray. This is a range of $\delta\theta = 2(\alpha_2 - \alpha_1)$, and we have

$$\delta\theta + \Delta\theta = \Delta\theta' \,. \tag{47}$$

Although θ' runs over a larger range than does θ, we can think of this larger range as counting the multiple reflected rays that can result from an incident ray with a given value of θ. This conclusion will continue to hold if we have more than two straight line segments. We can approximate any curve by a sequence of line segments. In general, the angle $\Delta\theta'$ subtended by the curve differs from the range of angle of incident rays, $\Delta\theta$, and if the curve is convex toward the point of interest, $\Delta\theta < \Delta\theta'$. At first sight, one might think that an emmeration of the independent modes should involve an integration over θ. This, however, fails to account for the multiple reflected rays, which are correctly counted if we instead integrate on θ'.

As we vary θ through its range of $-\pi < \theta \leq \pi$ (Note that here θ increases in the clockwise direction.), we have six possibilities:

$$
\begin{array}{cl}
-\pi < \theta < 2\alpha_1 - \pi & \text{incident ray only} \\
2\alpha_1 - \pi < \theta < \theta'_1 + 2\alpha_2 - \pi & \text{1 reflected ray} \\
\theta'_1 + 2\alpha_2 - \pi < \theta < \theta'_1 + 2\alpha_1 - \pi & \text{2 reflected rays} \\
\theta'_1 + 2\alpha_1 - \pi < \theta < \theta'_2 + 2\alpha_2 - \pi & \text{1 reflected ray} \\
\theta'_2 + 2\alpha_2 - \pi < \theta < \pi - \theta'_2 & \text{incident ray only} \\
\pi - \theta'_2 < \theta \leq \pi & \text{no rays.}
\end{array}
$$

In the latter case the incident ray fails to reach the point of interest because it is blocked by the mirror. Note, however, that the reflected rays exactly compensate for the missing incident rays in the sense that if we add up a weighted sum of the angle ranges with reflected rays, it is equal to the range with no rays. This observation is the justification for Eq. (6). The number of incident plus reflected rays in the presence of the boundary is the same as the number of incident rays in its absence.

One might ask whether it is important also to include the interference terms between the multiply refelcted rays. After all, the dominant contribution near the focus of a parabolic mirror comes from such an interference term. It is indeed true that if one wishes to compute a quantity such as $\langle \mathbf{E}^2 \rangle$ in the geometry of Fig. 4, we would need to include the interference terms. However, one should not expect to obtain an anomalously large result, but rather one of order r^{-4}, where r is the distance to the nearest boundary. This follows from the fact that the formula for $\Delta\ell$, the analog of Eq. (29) will be of the form of a product of r times a dimensionless angular dependent function.

4.2 Evaluation of Singular Integrals

We have derived expressions, such as Eqs. (30) and (32), for renormalized quantities near the focus of a parabolic mirror. Recall that we are dealing with a situation where there are two reflected rays for a single incident ray. Here θ'_1 is the angle of one of these rays, and the angle of the other, θ'_2 is understood to be a function of θ'_1. However, the integrals in question are singular at the point that $\theta'_1 = \theta'_2$. The singularity may be removed by an integration by parts [6, 7, 8]. We rewrite the integrand using relations such as

$$\frac{1}{x^2} = -\frac{1}{2}\frac{d^2}{dx^2} \ln x^2 \tag{48}$$

and

$$\frac{1}{x^4} = -\frac{1}{12}\frac{d^4}{dx^4} \ln x^2 \,. \tag{49}$$

Next we perform repeated integrations by parts until we have only an integral with a logarithmic singularity in the integrand, plus possible surface terms. Thus

$$\int dx\,\frac{f(x)}{x^2} = -\frac{1}{2}\int dx\,\ln x^2\,\frac{d^2 f(x)}{dx^2}\,, \tag{50}$$

and

$$\int dx\,\frac{f(x)}{x^4} = -\frac{1}{12}\int dx\,\ln x^2\,\frac{d^4 f(x)}{dx^4}\,, \tag{51}$$

provided that the function $f(x)$ is regular at $x = 0$ and the surface terms vanish.

In our case, the integration on θ'_1 ranges over those values of θ' for which there are multiple reflected rays. Within the geometric optics approximation, the integrand would seem to drop precipitously to zero at the end point of this interval. If one were to go beyond this approximation, the sudden drop would be smeared out over an interval corrresponding to about one wavelength. Thus we can think of our integrand as being an approximation to a function which, along with its derivatives, vanishes smoothly at the endpoints. If so, then we should be able to ignore the surface terms. In any case, we will here make the assumption that the surface terms can be ignored, and the singular integrands replaced by integrands with an integrable logarithmic singularity. The integration by parts procedure will be illustrated explicitly in the next section.

5 Results for Mirrors Slightly Larger than the Critical Size

As we found above (See Fig. 2.), there is a critical size which a parabolic mirror must have before we find large vacuum effects near the focus. The critical case is that of a mirror which subtends an angle of $\pi/3$ in either direction from the axis of symmetry (the x-axis in Fig. 1). In order to evaluate the integrals in Eqs. (30) and (32), we need to solve Eq. (23) for θ' in terms of θ, and then express one root θ'_2 as a function of the other, θ'_1. In general, this is difficult to do in closed form. There is, however, one case in which an analytic approximation is possible. This is when the size of the mirror is only slightly greater than the critical value. Let the angle subtended by the mirror be $\pi/3 + \xi_0$, where $\xi_0 \ll 1$. In this case, we can expand the needed quantities in terms of power series. Note that now both roots for θ' will be close to $\pi/3$, so let $\theta' = \pi/3 + \xi$ and expand Eq. (23) in powers of ξ to find (This and other calculations in this section were performed using the computer algebra program MACSYMA.)

$$\theta = \frac{3\sqrt{3}}{4} - \frac{3\sqrt{3}}{4}\xi^2 + \frac{1}{4}\xi^3 + \frac{3\sqrt{3}}{16}\xi^4 - \frac{1}{16}\xi^5 - \frac{11\sqrt{3}}{480}\xi^6 + \cdots\,. \tag{52}$$

Let $\theta'_1 = \pi/3 + \xi_1$ and $\theta'_2 = \pi/3 + \xi_2$. Assume a power series expansion for ξ_2 in terms of ξ_1. Next we equate the right-hand-side of Eq. (52) with $\xi = \xi_1$ to that with $\xi = \xi_2$ and iteratively solve for the coefficients in the expansion of ξ_2. The result is

$$\xi_2 = -\xi_1 + \frac{\sqrt{3}}{3}\xi_1^2 - \frac{1}{27}\xi_1^3 + \frac{35\sqrt{3}}{972}\xi_1^4 - \frac{97}{2916}\xi_1^5 + \cdots\,. \tag{53}$$

Our next task is to use this expansion to compute the integrands in Eqs. (30) and (32). First rewrite these expressions as

$$\begin{aligned} \langle \varphi^2 \rangle_{pr} &= -\frac{1}{8\pi^2 a^2} \int_{-\xi_0}^{\xi_0} d\,\xi_1 \frac{1}{[\cos(\frac{\pi}{3}+\xi_1) - \cos(\frac{\pi}{3}+\xi_1)]^2} \\ &= \frac{1}{16\pi^2 a^2} \int_{-\xi_0}^{\xi_0} d\,\xi_1 \ln {\xi_1}^2 \frac{d^2}{d\xi_1^2} \left\{ \frac{\xi_1^2}{[\cos(\frac{\pi}{3}+\xi_1) - \cos(\frac{\pi}{3}+\xi_1)]^2} \right\}, \end{aligned} \tag{54}$$

and

$$\begin{aligned} \langle \mathbf{E}^2 \rangle_{pr} &= \frac{3}{4\pi^2 a^4} \int_{-\xi_0}^{\xi_0} d\,\xi_1 \frac{1}{[\cos(\frac{\pi}{3}+\xi_1) - \cos(\frac{\pi}{3}+\xi_1)]^4} \\ &= -\frac{3}{48\pi^2 a^4} \int_{-\xi_0}^{\xi_0} d\,\xi_1 \ln {\xi_1}^2 \frac{d^4}{d\xi_1^4} \left\{ \frac{\xi_1^4}{[\cos(\frac{\pi}{3}+\xi_1) - \cos(\frac{\pi}{3}+\xi_1)]^4} \right\}. \end{aligned} \tag{55}$$

Note that we have introduced a factor of $\frac{1}{2}$ to compensate for overcounting of pairs of reflected rays, and then used the integrations by parts procedure discussed in the previous section. Next we use Eq. (53) to write

$$\frac{\xi_1^2}{[\cos(\frac{\pi}{3}+\xi_1) - \cos(\frac{\pi}{3}+\xi_2)]^2} = A_0 + A_1\xi_1 + A_2\xi_1^2 + \cdots, \tag{56}$$

and

$$\frac{\xi_1^4}{[\cos(\frac{\pi}{3}+\xi_1) - \cos(\frac{\pi}{3}+\xi_2)]^4} = B_0 + B_1\xi_1 + B_2\xi_1^2 + B_3\xi_1^3 + B_4\xi_1^4 + \cdots. \tag{57}$$

We see, that to leading order in ξ_0, the dominant contribution to $\langle \varphi^2 \rangle$ comes from the coefficient A_2, which is given by

$$A_2 = \frac{23}{324}. \tag{58}$$

This leads to our final result

$$\langle \varphi^2 \rangle_{pr} \approx -\frac{23}{648\pi^2 a^2}\, \xi_0(1 - \ln \xi_0) + O(\xi_0^2 \ln \xi_0). \tag{59}$$

Similarly, the leading contribution to $\langle \mathbf{E}^2 \rangle_{pr}$ comes from

$$B_4 = \frac{4051}{2^4 3^8 5}, \tag{60}$$

and is

$$\langle \mathbf{E}^2 \rangle_{pr} \approx \frac{4051}{2^2 3^7 5 \pi^2 a^4}\, \xi_0(1 - \ln \xi_0) + O(\xi_0^2 \ln \xi_0) \approx \frac{9.38 \times 10^{-3}}{a^4}\, \xi_0(1 - \ln \xi_0). \tag{61}$$

First we note that the leading contributions to both quantites diverge as $a \to 0$, that is, as one approaches the focus. This provides the justification of the geometric optics approximation. The modes which give the dominant contribution are those whose wavelengths are of order a, small enough that geometric optics is valid. Next we note that $\langle\varphi^2\rangle_{pr}$ diverges negatively, but $\langle\mathbf{E}^2\rangle_{pr}$ and the energy density for the scalar and electromagnetic fields diverge positively.

The above results apply in the case of a parabola of revolution; for the case of a parabolic cylinder we have

$$\langle\varphi^2\rangle_{pc} \approx -\frac{23}{972\pi^3 a^2}\,\xi_0(1-\ln\xi_0)\,, \tag{62}$$

and

$$\langle\mathbf{E}^2\rangle_{pc} \approx \frac{8102}{3^8 5^2 \pi^3 a^4}\,\xi_0(1-\ln\xi_0) \approx \frac{1.59\times10^{-3}}{a^4}\,\xi_0(1-\ln\xi_0)\,. \tag{63}$$

Note that all of the results in this section depend upon what is happening in a thin band centered on $\theta' = \pi/3$. The remainder of the mirror, that that for which $\theta' < \pi/3 - \xi_)$, does not even have to be present.

6 Observable Consequences?

Now we face the question of whether the amplified vacuum fluctuations are actually observable. The calculations given above indicate that the energy density and squared fields are singular at the focus of a perfectly reflecting parabolic mirror. However, the approximation of perfect reflectivity must break down at frequencies higher than the plasma frequency of the material in question . So long as the plasma wavelength λ_P is short compared to the size of the mirror, there is an intermediate regime in which geometric optics is valid. We simply must restrict the use of the geometric optics results to values of a larger than λ_P.

The quantity which is most easily observable is $\langle\mathbf{E}^2\rangle$, as it is linked to the Casimir force on an atom or a macroscopic particle. If the atom or particle has a static polarizability α, then the interaction energy with a boundary is

$$V = -\frac{1}{2}\,\alpha\,\langle\mathbf{E}^2\rangle\,. \tag{64}$$

Here we are assuming that the modes which give the dominant contribution to $\langle\mathbf{E}^2\rangle$ have frequencies below that at which a dynamic polarizability must be used. For a perfectly conducting parallel plate,

$$\langle\mathbf{E}^2\rangle_{\rm plate} = \frac{3}{16\,\pi^2\,z^4} \approx \frac{1.90\times10^{-2}}{z^4}\,, \tag{65}$$

where z is the distance to the plate. If we insert this expression into Eq. (64), then the result is the Casimir-Polder potential [9] for the interaction of an atom in its ground state with the plate. It is a good approximation when z is large compared to the wavelength associated with the transition between the ground state and the first excited state. The $1/z^4$ distance dependence of the Casimir-Polder potential was experimentally confirmed by Sukenik *et al* [10]. If we compare Eq. (65) with Eq. (61) or Eq. (63), we see that the mean squared electric field near the focus of a parabolic mirror is only slightly less than that at the same distance from a flat plate. Given that the latter has actually been observed, it is possible that the inhanced fluctuations near the focus are also observable by techniques similar to those by Sukenik *et al.*

The basic method used in the Sukenik *et al* experiment is to look for the effects of the deflection of a beam of atoms as it passes near a pair of plates. We can give a general estimate of the size of this type of deflection which applies whenever there is a mean squared electric field which varies as the inverse fourth power of a length scale. Let

$$\langle \mathbf{E}^2 \rangle = \frac{\Lambda}{a^4}\,, \tag{66}$$

where a is the length scale and Λ is a dimensionless constant. We assume that an atom has an interaction of the form of Eq. (64). The resulting force, $F = -\partial V/\partial a$, will cause a deflection Δa in the atom's position in a time t, where

$$\frac{\Delta a}{a} = 0.25 \left(\frac{\Lambda}{10^{-3}}\right) \left(\frac{\alpha}{\alpha_{Na}}\right) \left(\frac{m_{Na}}{m}\right) \left(\frac{1\mu\mathrm{m}}{a}\right)^6 \left(\frac{t}{10^{-3}s}\right)\,. \tag{67}$$

Here $m_{Na} = 3.8 \times 10^{-23}$gm and $\alpha_{Na} = 3.0 \times 10^{-22}\mathrm{cm}^3$ denote the mass and polarizability of the sodium atom, respectively. (Note that polarizability in the Lorentz-Heaviside which we use is 4π times that in Gaussian units.) If t is of order $10^{-3}s$ (the time needed for an atom with a kinetic energy of order 300K to travel a few centimeters), and z is of order 1μm, the fractional deflection is significant. Recall that in our case

$$\Lambda = \begin{cases} 9.38 \times 10^{-3}\,\xi_0(1 - \ln \xi_0)\,, & \text{parabola of revolution} \\ 1.59 \times 10^{-3}\,\xi_0(1 - \ln \xi_0)\,, & \text{parabolic cylinder.} \end{cases} \tag{68}$$

Thus it may be possible to observe the force on atoms near the focus.

Another possible way to observe this force might be to levitate the atoms in the Earth's gravitational field. (A rather different form of levitation by Casimir forces was proposed in Ref. [2].) If one equates the force on atom at a distance a from the focus to its weight, the result can be expressed as

$$a = \left(\frac{2\Lambda\alpha}{mg}\right)^{\frac{1}{5}} = 0.55\mu\mathrm{m} \left[\left(\frac{\Lambda}{10^{-3}}\right) \left(\frac{\alpha}{\alpha_{Na}}\right) \left(\frac{m_{Na}}{m}\right)\right]^{\frac{1}{5}}\,. \tag{69}$$

Given that this formula applies for $a > \lambda_P$ and that $\lambda_P \approx 0.1\mu$m for many metals, it seems possible that levitation near the focus is possible. Of course, atoms will only be trapped if their temperature is sufficiently low. The required temperature can be estimated by setting the thermal energy $\frac{3}{2}kT$ equal to the magnitude of the potential energy V. The result is

$$T = 2 \times 10^{-5} K \left(\frac{\Lambda}{10^{-3}}\right) \left(\frac{\alpha}{\alpha_{Na}}\right) \left(\frac{0.1\mu\mathrm{m}}{a}\right)^4\,. \tag{70}$$

Thus for a of the order of a few times 0.1μm, the required temperature is larger than the temperatures of the order of $10^{-7}K$ which have already been achieved for laser cooled atoms [11, 12].

Another possibility might be the use of atom interferometry. Atoms traveling for a time t parallel to and near the focus of a parabolic cylinder will acquire a phase shift of

$$\Delta\phi = \frac{t}{2}\,\alpha\,\langle \mathbf{E}^2 \rangle_{pc} = 7.2 \times 10^{-2} \left(\frac{\alpha}{\alpha_{Na}}\right) \left(\frac{1\mu\mathrm{m}}{a}\right)^4 \left(\frac{t}{10^{-3}s}\right) \xi_0(1 - \ln \xi_0)\,. \tag{71}$$

If it is possible to localize the atoms to within a few μm of the focus, then the accumulated phase shift for reasonable flight times would seem to be within the currently attainable sensitivities of the order of 10^{-4} radians [12].

7 Discussion and Conclusions

In this paper we have argued that a parabolic mirror is capable of focusing the vacuum modes of the quantized electromagnetic field and creating large physical effects near the mirror's focus. Just as the mirror can focus a beam of light, it can focus something even in the absence of incoming light. This might be dubbed "focusing a beam of dark" [13]. The manifestation of this focusing is a growth in the energy density and mean squared electric field as the focus is approached. In the idealized case of a perfectly reflecting mirror, these quantities diverge as the inverse fourth power of the distance from the focus. For a real mirror, the growth is expected to saturate at distances of the order of the plasma wavelength of the mirror.

The most readily observable consequence of the focused vacuum fluctuations is enhanced Casimir forces on atoms or other particles near the focus. The sign of the force is such as to draw particles into the vicinity of the focus. Estimates given in the previous section indicate that the magnitude of this effect may be large enough to be observable.

The calculations presented in this paper were based on the geometric optics approximation in which only short wavelenth modes are considered. The justification of this approximation is self-consistency: the large effects near the focus can only come from the short wavelength modes for which the approximation should be a good one.

In order to simplify the calculations, we made two restrictions on the geometry. The first is that we have assumed that the point at which the mean squared field quantites are measured lies on the symmetry axis of the parabola (the x-axis). The second is that the mirror be only slightly larger than the critical angle of $\pi/3$ at which vacuum focusing begins. (This is the assumption that $\xi_0 \ll 1$, made in Sect. 5.) It is of interest to remove both of these restiction, which we hope to do in a future work.

Acknowledgement: We would like to thank Paul Davies for helpful discussions. This work was supported in part by the National Science Foundation under Grant PHY-9800965.

REFERENCES

[1] L.H. Ford, Phys. Rev. A **48**, 2962 (1993).

[2] L.H. Ford, Phys. Rev. A, **58**, 4279 (1998), quant-ph/9804055.

[3] L.H. Ford, Phys. Rev. D **38**, 528 (1988).

[4] S. Hacyan, R. Jáuregui, F. Soto, and C. Villarreal, J. Phys. A **23**, 2401 (1990).

[5] I.S. Gradshteyn and I.M. Ryzhik, *Table of Integrals, Series, and Products* (Academic Press, New York, 1980), 3rd Edition.

[6] K.T.R. Davies and R.W. Davies, Can. J. Phys. **67**, 759 (1989); K.T.R. Davies, R.W. Davies, and G. D. White, J. Math. Phys. **31**, 1356 (1990).

[7] D.Z. Freedman, K. Johnson and J.I. Latorre, Nucl. Phys. **B371**, 353 (1992).

[8] C.-H. Wu and L. Ford, Phys. Rev. D **60**, 104013 (1999), gr-qc/9905012.

[9] H.B.G. Casimir and D. Polder, Phys. Rev. **73**, 360 (1948).

[10] C.I. Sukenik, M.G. Boshier, D. Cho. V. Sandoghar, and E.A. Hinds, Phys. Rev. Lett. **70**, 560 (1993).

[11] W.D. Phillips, Rev. Mod. Phys. **70**, 721 (1998).

[12] C.E. Wineland, D.F. Pritchard, and D.J. Wineland, Rev. Mod. Phys. **71**, S253 (1999).

[13] We are grateful to Paul Davies for suggesting this phrase to us.